SCIENTIFIC REPORTS

OPEN

SUBJECT AREAS:
CANCER IMAGING
DRUG DELIVERY
DRUG DEVELOPMENT

Received
26 February 2014

Accepted
11 August 2014

Published
10 September 2014

Correspondence and requests for materials should be addressed to H.L. (hyoyoung@skku.edu)

Cancer Therapy Using Ultrahigh Hydrophobic Drug-Loaded Graphene Derivatives

Surajit Some[1], A-Ryeong Gwon[4], Eunhee Hwang[1], Ga-hee Bahn[4], Yeoheung Yoon[1,2], Youngmin Kim[1], Seol-Hee Kim[4], Sora Bak[1], Junghee Yang[1], Dong-Gyu Jo[4] & Hyoyoung Lee[1,2,3]

[1]National Creative Research Initiative, Center for Smart Molecular Memory, Department of Chemistry, Sungkyunkwan University, 2066 Seoburo, Jangan-Gu, Suwon, Gyeonggi-Do 440-746, Republic of Korea, [2]Department of Energy Science, Sungkyunkwan University, 2066 Seoburo, Jangan-Gu, Suwon, Gyeonggi-Do 440-746, Republic of Korea, [3]SKKU Advanced Institute of Nano Technology (SAINT), Sungkyunkwan University, 2066 Seoburo, Jangan-Gu, Suwon, Gyeonggi-Do 440-746, Republic of Korea, [4]School of Pharmacy, Sungkyunkwan University, 2066 Seoburo, Jangan-Gu, Suwon, Gyeonggi-Do 440-746, Republic of Korea.

This study aimed to demonstrate that curcumin (Cur)-containing graphene composites have high anticancer activity. Specifically, graphene-derivatives were used as nanovectors for the delivery of the hydrophobic anticancer drug Cur based on pH dependence. Different Cur-graphene composites were prepared based on polar interactions between Cur and the number of oxygen-containing functional groups of respective starting materials. The degree of drug-loading was found to be increased by increasing the number of oxygen-containing functional groups in graphene-derivatives. We demonstrated a synergistic effect of Cur-graphene composites on cancer cell death (HCT 116) both *in vitro* and *in vivo*. As-prepared graphene quantum dot (GQD)-Cur composites contained the highest amount of Cur nano-particles and exhibited the best anticancer activity compared to the other composites including Cur alone at the same dose. This is the first example of synergistic chemotherapy using GQD-Cur composites simultaneous with superficial bioprobes for tumor imaging.

With the recent rapid progress in nano-biotechnology, the use of nanomaterials as drug carriers for cancer therapy is receiving increased attention[1,2]. Carbon nanostructures (e.g., graphene-derivatives and graphene quantum dots (GQDs)) exhibit favourable biocompatibility with low toxicity, excellent physical properties, a surface amenable to modification, improved multifunctionality, and compatibility with conventional graphene technology[2,3]. In particular, the use of graphene-derivatives is very promising for a wide range of biological applications, including the recent development of GQD-based bioprobes for tumor imaging[4,5]. However, existing drug carriers including proteins, amphiphilic block copolymers, lipids, and inorganic nanoassemblies are associated with a number of drawbacks including undesirable burst drug release and premature drug leakage due to limited stability[6,7]. It was recently demonstrated that graphene materials can be loaded with aromatic ring-containing anticancer drugs such as doxorubicin (DOX) and camptothecin (CPT) with ultrahigh efficiency[3,8–12]. Graphene-oxide-derivative-Cur composites have also been reported to have anticancer activity[13,14], but they are neither very effective nor easily produced. Indeed, their use has not been demonstrated in a real application, i.e., treating tumours or inhibition of tumor growth, and their drug-loading capability is low, suggesting that they are not ideal for clinical applications. There have also been reports of graphene quantum dot-loaded drugs, but they are not efficient and have not been shown to be useful for any real applications such as tumor treatment[15,16]. The use of graphene-based nanomaterials deserves attention in order to overcome this physiological barrier because these nanomaterials exhibit excellent adsorption properties in the bloodstream[17–19]. Therefore, graphene-based drug delivery nanosystems that are compatible with physiological environments are very desirable. As a result, the use of graphene in biomedicine is being investigated[20,21]. Of particular interest, recent studies have shown that graphene-derivatives exhibit excellent catalytic performance owing to the high surface area for producing polar interactions with oxygen-containing functional groups, which is also a significant factor for the enhancement of drug-loading capacity[3,9,22]. In the search for pharmaceutical agents for the treatment of cancer, many different hydrophobic drugs such as Cur have been found to be highly effective against various carcinomas. However, the low solubility of these hydrophobic drugs in aqueous media hinders their clinical use for the treatment of cancer.

Motivated by the significant features of graphene, we investigated the effectiveness of graphene-derivative-based drug nano-composites for cancer therapy using graphene oxide (GO), double-oxidized graphene oxide (DGO), and GQDs as novel nanovectors for delivery of the hydrophobic anticancer drug Cur (Figure 1). Our results represent the first comprehensive study of a cancer therapy using ultrahigh hydrophobic drug-loaded graphene derivatives based on the number of oxygen-containing functional groups and delivered based on pH dependence. We hypothesized that the increase in the number of oxygen-containing groups on the surface of graphene derivatives would lead to increased attachment of Cur. We also assumed that the oxygen-containing functional groups would interact effectively with hydrophobic Cur in basic medium to assist in formation of *in-situ* nanoparticles of Cur and the production of DGO-Cur composites with increased anticancer activity. In addition, GQDs were assumed to produce GQD-Cur composites with very high anticancer activity, where the large amount of Cur was due to the presence of a large surface area with many oxygen-containing functional groups.

Graphene-derivative Cur composites were quickly prepared according to a new, simple, and easy method in which Cur was effectively attached to the surface of graphene derivatives. Importantly, experiments performed both *in vitro* and *in vivo* demonstrated that graphene derivative-based nano-composites were highly efficacious as cancer therapeutics. Among the graphene derivatives, GQD was the best composite, carrying a large amount of Cur and serving as a bioprobe for tumor imaging. As per our hypothesis, the amount of drug loading increased with an increasing number of oxygen-containing functional groups of graphene derivatives. Remarkably, GQDs exhibited an ultrahigh drug-loading capacity of ~40,800 mg/g, which is the highest value ever reported for a nanomaterial-based carrier.

Results

GO sheets were synthesized from graphite powder using a modified Hummer's method (Bay carbon, SP-2) and purified as described previously[23]. DGO sheets were synthesized according to a previously reported procedure[24]. GQDs containing additional oxygen functionalities were synthesized as described previously[4].

Preparation and characterization of graphene composites. On the basis of XPS analyses, the as-made GO had a low C/O ratio (2.2) (Supplementary Figure S1). The resulting DGO exhibited a low C/O ratio of ~1, corresponding to an increase in the oxygen content of the DGO nanosheets[24]. Likewise, the as-made GQDs exhibited the lowest C/O ratio (Supplementary Figure S1), indicating that the GQDs also contained the largest amount of oxygen-containing functional groups. Finally, we prepared Cur-loaded composites of GO, DGO and GQD, which were then characterized by Fourier transform infrared spectroscopy (FT-IR), UV-vis absorption spectra, and scanning electron microscopy (SEM) analyses. Using FTIR spectroscopy (Figure 2a), we determined the characteristic absorption patterns of the different Cur functional groups on the graphene-derivatives and also confirmed the physical attachment of Cur to graphene derivatives by polar interaction. As shown in Figure 2a, the FTIR spectra revealed oxygen functionalities in GO at 3530 (O-H stretching vibrations), 1729 (C=O stretching vibrations), 1634 (C=C skeletal vibrations from unoxidized graphitic diamonds), and 1058 cm^{-1} (C-O stretching vibrations)[25]. In addition, after double oxidation of GO, which produced the DGO derivative, the peak ratios of 3529 and 1737 cm−1 (O-H and C=O stretching vibrations, respectively) with 1116 cm^{-1} (aromatic C-O stretching vibrations) decreased, indicating that these GOs were functionalized with more oxygen-containing groups. The spectrum in Figure 2a shows the presence of C=C, C−O, C=O, and COOH bonds, indicating that the GQDs were functionalized with hydroxyl, carbonyl, and carboxylic acid groups, respectively[15]. Cur exhibited prominent peaks at 3510, 1510, 1276, 1152, and 959 cm^{-1} (Figure 2a) due to OH, C-O, C-H, aromatic C-O, and C-O-C stretching vibrations, respectively[26]. Likewise, the GO-Cur composite exhibited characteristic Cur absorption features at 1509, 1272 and 1153 cm^{-1}, which was similar to that of Cur alone. The other composites including DGO-Cur and GQD-Cur also exhibited characteristic peaks around 1509, 1275 and 1154 cm^{-1}, indicating

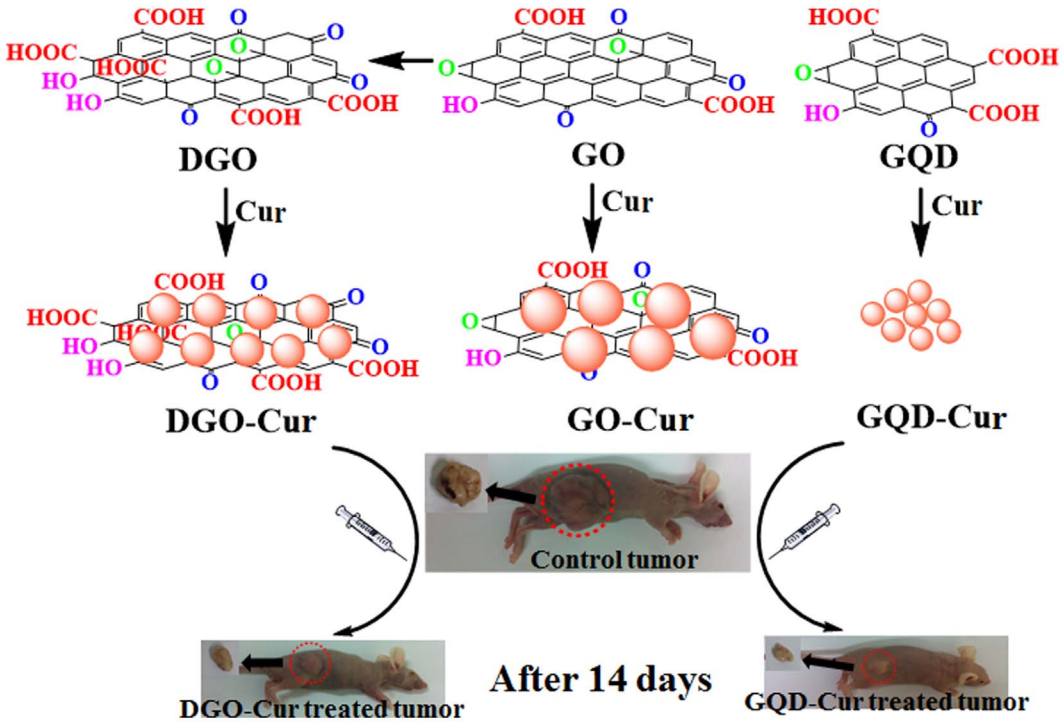

Figure 1 | Schematic diagram of the preparation of various curcumin-graphene composites (GO-Cur, DGO-Cur, and GQD-Cur) and their relative anticancer effects.

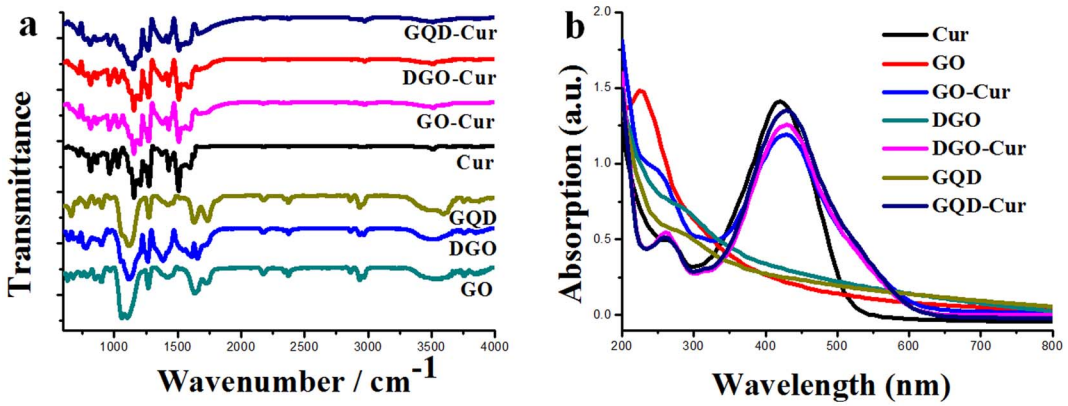

Figure 2 | FTIR and UV-vis spectra of different compounds. (a) FTIR spectra of GO, DGO, GQD, GO-Cur, DGO-Cur, GQD-Cur composites, and Cur. (b) UV-vis spectra of GO, DGO, GQD, GO-Cur, DGO-Cur, GQD-Cur composites, and Cur.

that they also contained Cur. The intensity of O-H stretching vibrations for all of the composites was decreased, indicating that Cur was successfully grafted onto GO, DGO and GQD.

The main UV-vis absorption peak of GO appeared at 226.5 nm[9] (Figure 2b). In the case of Cur alone, the absorption peak appeared at 419.2 nm[27], whereas the peaks for DGO and GQD appeared at 286 and 292 nm[28], respectively. After the composite formation of Cur with GO, DGO and GQD, we observed a red shift relative to the Cur peak. Specifically, the main absorption peaks of GO-Cur, DGO-Cur and GQD-Cur appeared in the UV-vis spectra at ~430 nm, an ~10 nm red shift compared with the peak for Cur only, indicating the formation of composites.

Scanning electron microscopy (SEM) was used to determine the surface morphologies of the various graphene derivatives (Figure 3). GOs exhibited thin, wrinkled GO sheets in SEM images (Figure 3a). Likewise, the SEM-images of GO-Cur indicated that Cur was physically attached to the GO surface. The average size of Cur nano-particles was ~150 nm, and SEM images of the GO-Cur composite showed that Cur molecules were fabricated on wrinkled GO sheets (Figure 3e). In addition, DGO sheets appeared to form after another oxidation of the as-made GO (Figure 3b). SEM images of DGO revealed a more wrinkled morphology compared with that of GO. Likewise, SEM images of the DGO-Cur composite (Figure 3f) showed that the DGO surface had more Cur nano-particles than did GO-Cur (Figure 3e)The average size of the Cur nano-particles was ~150 to ~120 nm. Figure 3c shows an SEM image of GQD, which revealed the presence of numerous round-shaped composites with an average size of ~100 nm (Figure 3g), and can be compared with Figure 3d, an SEM image of Cur alone. Thus, SEM provided evidence for the formation of the composites and also revealed *in-situ* formation of Cur nano particles, the size of which decreased with an increasing number of oxygen functional groups. Furthermore, the HRTEM image in Figure 3h shows that the synthesized GQDs were symmetrical. Size and morphology analysis indicated that the nano-sized GQDs had a diameter of 3–6 nm (Supplementary Figure S2) as measured by HRTEM. The HRTEM images of GQD-Cur also revealed round-shaped Cur-encapsulated GQD composites[29] that were relatively larger than GQD alone, with an average size of ~100 nm (Figure 3g).

GQD containing a larger number of oxygen functional groups was synthesized as described previously[4]. GQD exhibited excellent photoluminescence due to UV excitation (400 nm). Figure 4a shows the photoluminescent (PL) intensity of GQDs, indicating the concentration-dependent PL intensity of the GQDs at an emission wavelength of 512 nm. However, GQD formed composites with Cur, and the relative PL of those composites gradually decreased with increasing amount of Cur (Figure 4b), whereas Cur alone had no PL intensity (Supplementary Figure S3). With respect to the PL intensity described previously, sufficient fluorescence intensity of GQDs was observed for three days due to their low stability in aqueous solution[4]. Moreover, GQD has interesting pH-dependent PL behaviours; PL intensity decreases in solution with a high or low pH[30].

A cross-sectional view of the AFM image showed ~1 nm topographic heights, clearly illustrating the presence of a single layer of GQDs (Supplementary Figure S4). We also measured average size distributions of the GO and DGO by AFM images (Supplementary Figure S5). The chemically-synthesized GQDs were readily water-dispersible due to the presence of a large number of oxygen-containing functional groups, which was confirmed by FTIR. Free-standing graphene derivatives (as-made GO, DGO and GQD) at a concentration of 200 μg/mL were then mixed with 1 mg of Cur in alkaline aqueous solutions (~pH 9) under adequate stirring. The mixed solutions were initially turbid because of the poor aqueous dispersibility of pure Cur but gradually dissolved within a few minutes as the Cur nano-particles became increasingly adsorbed to the surfaces of graphene derivatives though interactions between Cur molecules and alkaline-mediated oxygen functional groups. Finally, clear solutions were observed because of the large amount of Cur nano-particles loaded onto the graphene-derivatives, forming GO-Cur, DGO-Cur, and GQD-Cur complexes. Centrifugation was carried out to dispose of residual Cur molecules that were not loaded onto the graphene derivatives. In brief, the as-prepared GO-Cur, DGO-Cur complexes were precipitated under centrifugation (14000 rpm, 20 min), while free Cur molecules remained in the supernatant because of their low molecular weight. Afterwards, the precipitate was collected and washed several times with DI water, while GQD-Cur complexes were collected by recrystallization of unattached Cur and evaporation of the resulting solution.

We next quantitatively studied the loading behaviours of Cur on graphene derivatives in acidic to basic environments covering a pH range of 5–9. The concentration of loaded Cur was determined by the calculation of free Cur (Figure 4c). We found that the amount of Cur bound to graphene derivatives was pH-dependent, and that the loading factors (defined as the graphene derivative/Cur weight ratio) were ~40.8, 38.8 and 20.8 for GQD-Cur, DGO-Cur and GO-Cur, respectively (Figure 4c). The loading amount of Cur gradually decreased from a high amount to a very low amount as the pH was reduced from 9 to 7.5 to 5 (Figure 4d). This trend was attributed to protonation and subsequent reduced interaction between Cur and graphene derivatives. A similar type of pH-dependent loading of nanomaterial-based nanocarriers has been previously reported[2]. Moreover, the Cur-loading efficiency was investigated for different initial Cur concentrations at a fixed concentration of graphene derivatives (200 μg/mL). As shown in Figure 4c, the Cur-loading on the graphene derivatives gradually increased with increasing initial concentration of Cur in neutral and basic environments (pH 7.5–9). Of

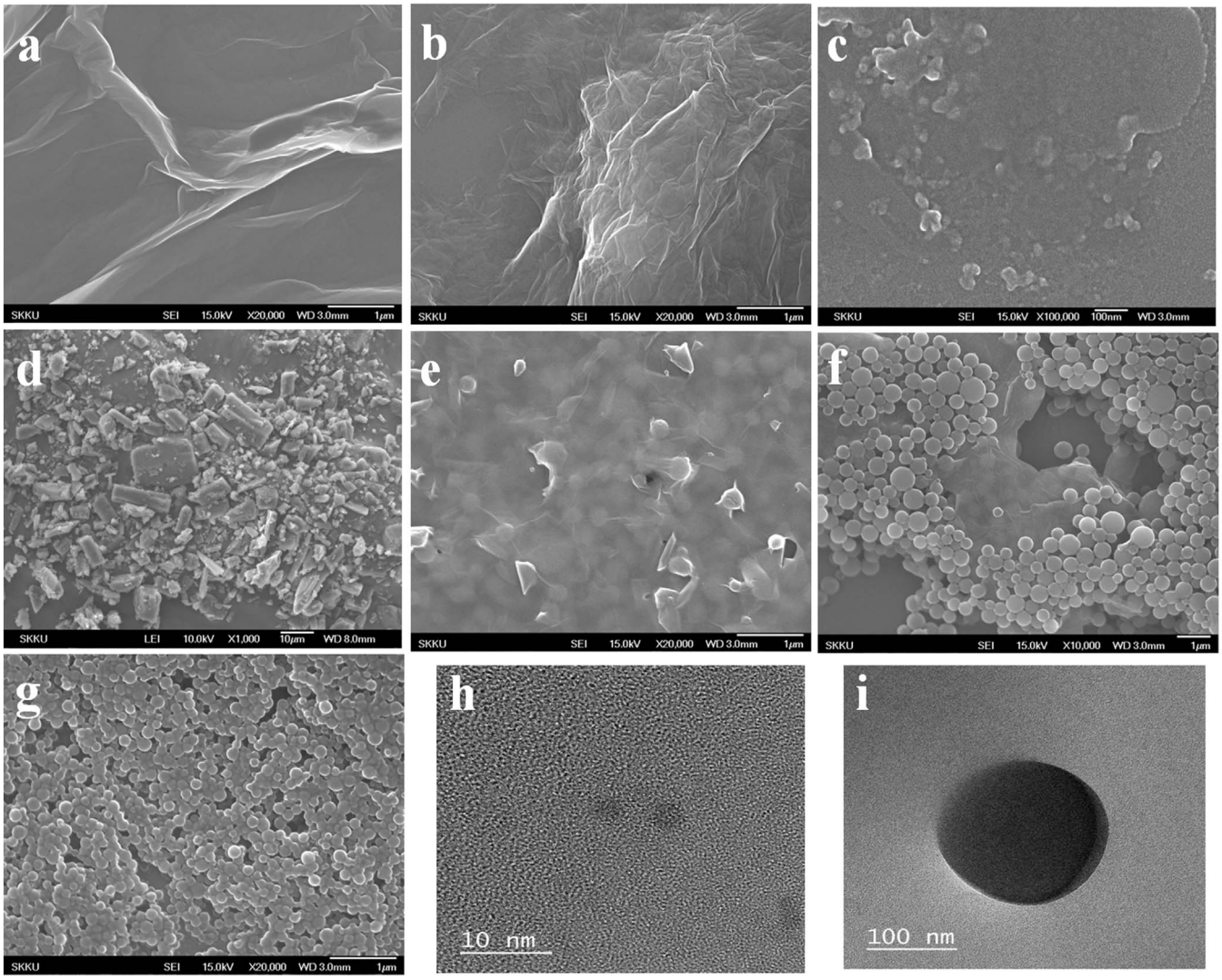

Figure 3 | SEM and TEM images of different materials. (a) SEM image of GO only. (b) SEM image of DGO only. (c) SEM image of GQD. (d) SEM image of Curcumin. (e) SEM image of the GO-Cur composite. SEM images of the DGO-Cur composite (f) and GQD-Cur composite (g). TEM images of GQD alone (h) and the GQD-Cur composite (i).

particular significance was that the loading capacity of Cur dramatically increased to 40,800 mg/g under optimal conditions for GQD (e.g., at pH 9 and a Cur of 1 mg). Based on our experimental data, we also concluded that GQD had a larger amount of Cur nano-particles than did GO or DGO.

Next, we investigated the Cur-releasing behaviour of the complexes prepared at pH 9. The concentration of the released Cur was determined by measuring free Cur. In particular, Cur molecules stacked on graphene derivatives remained stable in basic and near neutral buffers in which about ~9.8% to ~5% Cur was released from graphene derivatives at pH 7.5 or 9 in 24 h, respectively[31]. In sharp contrast, as much as ~85% of Cur was released from graphene derivatives after 24 h at ~pH 5 (Figure 4d) due to protonation and subsequent reduced interaction between Cur and graphene derivatives in acidic environments. It is well known that pH-dependent drug-loading and releasing properties are favourable for cancer therapy since the microenvironments of extracellular tumours tissues and intracellular lysosomes and endosomes are acidic[2], which may facilitate active drug release from the as-made composites.

Cell viability of the composites. To evaluate and compare the *in vitro* cytotoxicity of the composites, we analysed the effects of GO, DGO, GQD, Cur, and Cur loaded with GO, DGO and GQD on the cell viability of HCT 116 cells, a common human colon adenocarcinoma cell line. As expected, cell viability was greater than 90% for GO, DGO and GQD, indicating that the graphene derivatives were biocompatible (Figure 4e)[4,8]. As shown in Figure 4e, about 90% of cells were killed by the Cur composites at a concentration of 100 μg/mL. Among all of the composites tested, GQD-Cur was the most effective, killing more than 90% of cancer cells, while GO-Cur and DGO-Cur killed less than 90%. Specifically, the decrease in cancer cell viability with Cur alone was around 70%, which was low compared with other treatments under similar conditions. Importantly, the GQD-Cur composite was effective at low concentrations (6.125 μg/mL), killing 40% of cells. The increased cytotoxicity of the composite molecules compared with Cur alone was attributed to the high surface areas of GO, DGO and GQD, which enabled polar interactions of oxygen-containing functional groups to significantly enhance factors for drug-loading in the composites and/or to promote cytotoxicity of the drug composites by increasing cellular uptake of Cur upon formation of complexes with graphene derivatives. In addition, Cur in the composites formed small-sized nanoparticles (0.15 to less than 0.1 μm) in comparison to those in Cur alone (~1 μm) (Figure 3d), resulting in an increased number of reactive sites. It is worth noting that, in comparison to the high degree of cytotoxicity of the graphene derivative-Cur complexes,

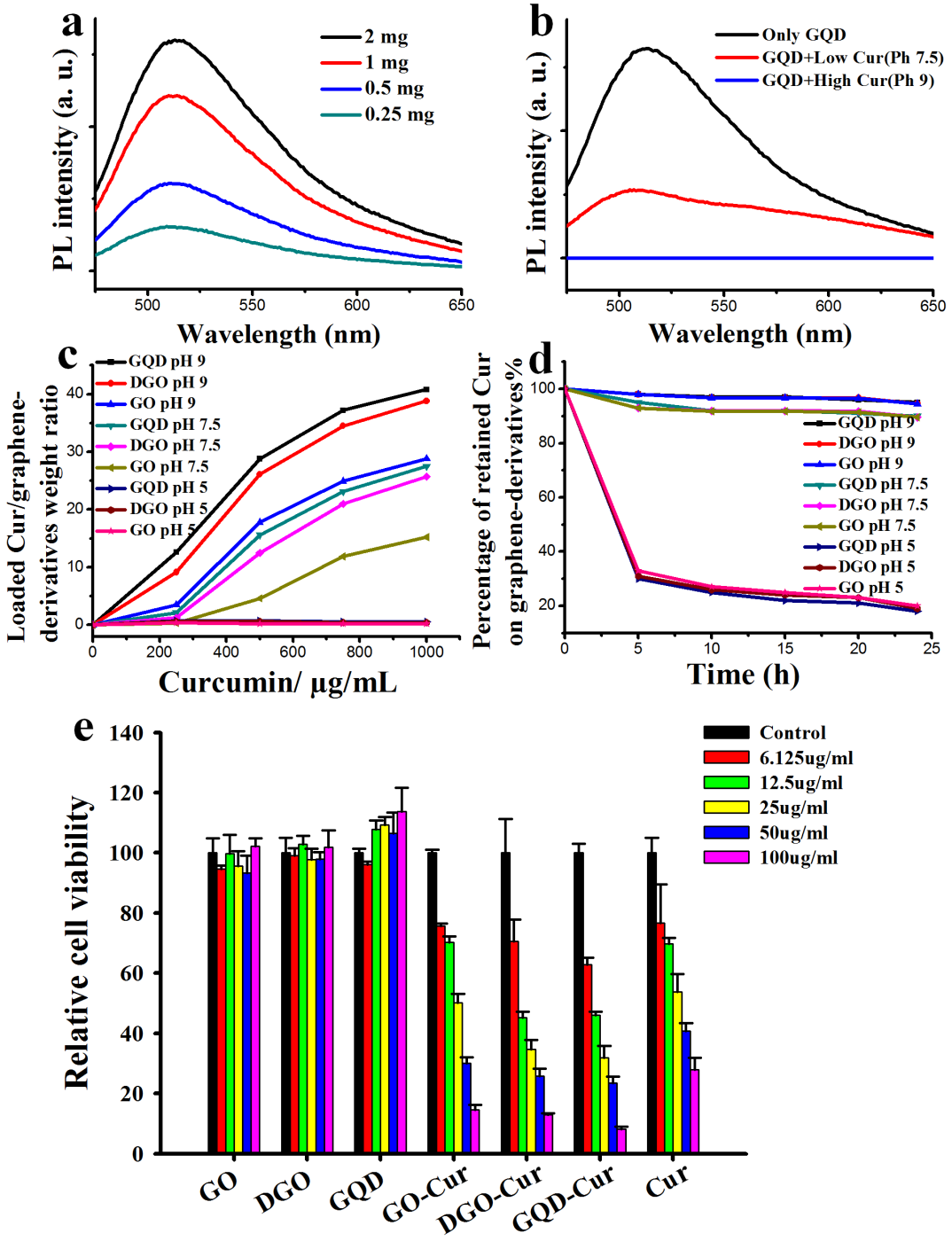

Figure 4 | Behaviours of the graphene-derivatives. (a) PL intensities of the GQDs at 512 nm, (b) PL intensities of GQDs alone and curcumin-loaded GQDs, (c) Quantification of various concentrations of curcumin loaded at different pH values (pH 5, 7.5, and 9). (d) Curcumin retained on GO, DGO and GQD versus time at constant pH (pH 5, 7.5, and 9). (e) *In vitro* concentration-dependent cell viability of HCT 116 cells. Cells were incubated with free GO, DGO, GQD, GO-Cur, DGO-Cur, GQD-Cur, and free Cur for 24 hrs.

cells incubated with pure graphene derivatives had high viability (>90%), suggesting that the graphene derivatives may serve as noncytotoxic drug nanocarriers owing to the favourable biocompatibility of graphene[8]. Lastly, cytotoxicity data was compiled to determine the mean growth-inhibitory concentrations (IC_{50}) of the composites (Table S1). To further assess cell viability, cells were stained with FITC conjugated anti-Annexin V Abs and propidium iodide (PI) (Figures 5a–i)[32]. The results suggest that a synergistic effect was achieved in our system. Specifically, we observed that treatment with GQD-Cur and DGO-Cur composites increased the HCT116 cells death, compared with cells treated with GO-Cur or Cur alone (Figure 5). We also did assess cell viability test with 4,6-diamidine-2-phenylindole dihydrochloride (DAPI) and imaged by a fluorescence microscope (Figures S6a–h). In Figure S6e–h, the condensed and/or fragmented nuclei are marked by arrows, providing the evidence of cell death[33]. Cur molecules were thus efficiently released from complexes distributed in cells because of the acidic environment (pH 5.0)[31]. Consequently, the graphene derivative-Cur complexes accumulated in cells may have enabled continuous Cur release in cancer cells, ensuring sufficient Cur accumulation in order to achieve adequate concentration to continually kill cancer cells[14].

***In vivo* tumor inhibition tests in the presence of different composites.** Given the outstanding *in vitro* synergistic effect between DGO-Cur and GQD-Cur complexes compared with Cur alone, we next investigated the *in vivo* therapeutic effects of composites in mice with HCT tumors on their back. Female nude mice with subcutaneous xenografts were divided into groups and were administrated a single intratumor dose of physiological saline, pure DGO and GQDs, free Cur, or DGO-Cur and GQD-Cur complexes, respectively. Six groups of tumor-bearing mice with six mice per group were used in our experiment. For mice injected with only Cur or the graphene derivative-Cur nano-complexes, we chose a concentration of 5 or 10 mg/kg, respectively. As expected, the graphene derivative-based nano-complexes in the tumor site provided favourable enhancement of the tumor therapy efficiency, whereby the stable and continual release of Cur from Cur-graphene composites effectively killed cancer cells and inhibited tumor growth. Quantitative measurement of the inhibition of tumor growth in terms of tumor volume change further confirmed the superior therapeutic efficacy of the graphene derivative-based nanocomposites. Figures 6a and S7 show the tumor volume measured for each group plotted as a function of time. The pink, red, and black lines in Figure 6a show the time-related increase in tumor volume for the three control groups treated with PBS, GQD, DGO alone, respectively. These tumors had average volumes (V, mm^3) of ~1000 (pink line), ~1027 (red line) or ~1100 (black line), respectively, after 14 days of treatment. While tumor growth was initially inhibited to some extent (blue line) in the control group treated with free Cur, tumor size did eventually increase (Figure 6a). In striking contrast, the DGO-Cur and GQD-Cur groups exhibited a remarkable inhibition of tumor growth, with GQD-Cur- and DGO-Cur-treated mice surviving more than 14 days with almost no observable increase in tumor size (yellow and green lines in Figure 6a). Importantly, the findings for GQD-Cur- and DGO-Cur-treated mice were consistent with other reported procedures for tumor growth using nanomaterial-based drug carriers for cancer therapy. According to our *in vivo* results, the

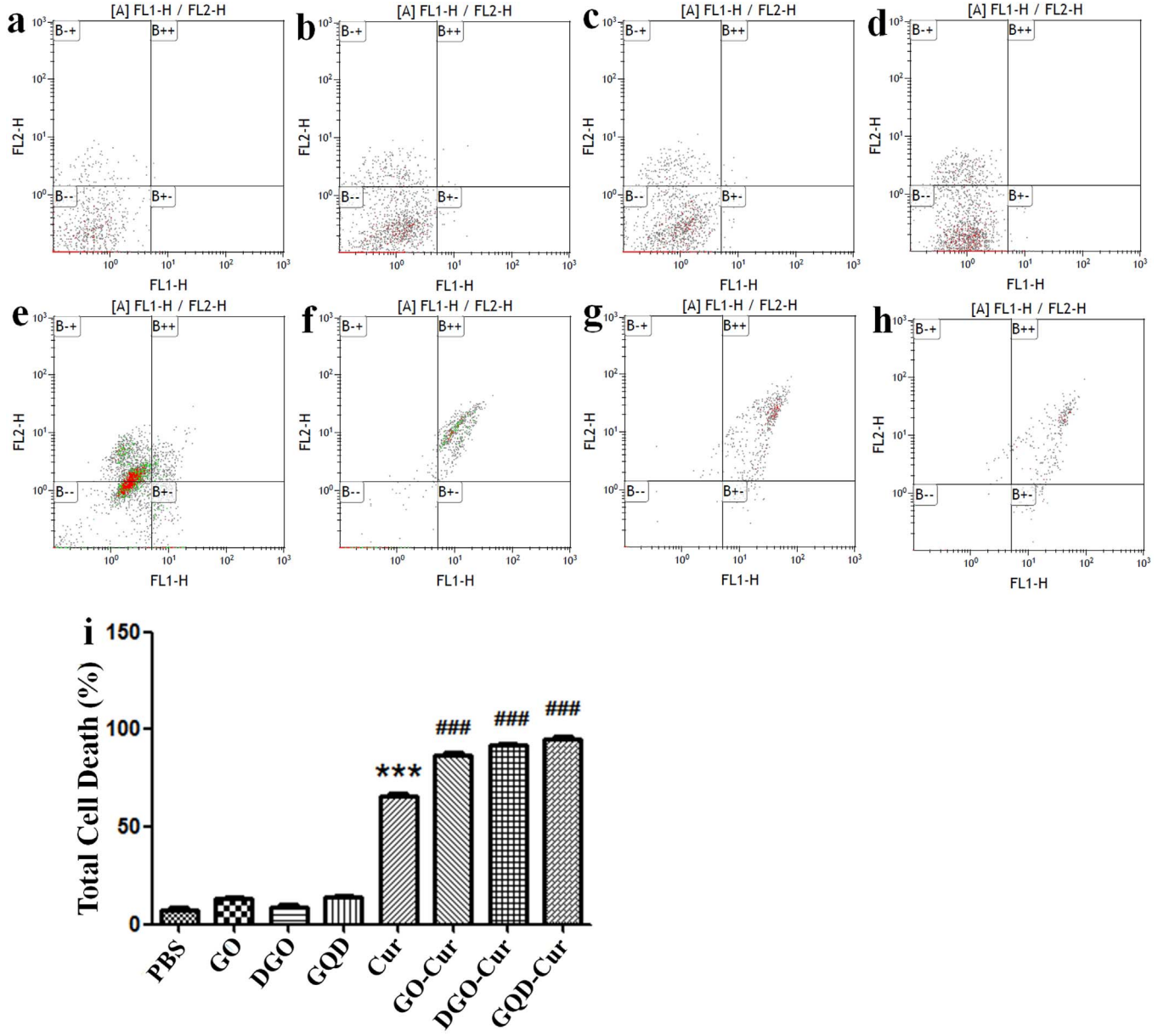

Figure 5 | Representative total cell death images obtained by annexin V Abs and propidium iodide co-staining with flow cytometric analysis. HCT 116 cells after treatment with (a) PBS, (b) GO, (c) DGO, (d) GQD, (e) Cur, (f) GO-Cur, (g) DGO-Cur, (h) GQD-Cur, and (i) total cell death score graph. Values are means ± SEM (n = 3). ***$P < 0.001$ versus PBS; $^{###}P < 0.001$ versus Curcumin. (One-way ANOVA).

GQD-Cur complex was also more effective than the DGO-Cur complex.

Intratumoral GQD distribution in mice after injection of GQD or the GQD-Cur complex at 10 mg/kg was analysed by non-invasive imaging using an Optix *in vivo* imaging system (Optix MX3, ART Advanced Research Technologies INC, Canada)[4]. As shown in Figure 6e, no GQD fluorescence was detected in mice treated with PBS (control sample); in comparison, distinct GQD fluorescence signals were observed in the tumor injected with only GQD or GQD-Cur. However, after the release of Cur from the composite, the remaining GQD exhibited a fluorescence signal, while the GQD-Cur nano-composite had no fluorescence signal. Taken together, these results demonstrate that GQD nano-composites can be used for treating cancer and simultaneously as a bioprobe for tumor imaging. Indeed, according to a previous report, nanosized GQDs accumulated in the tumor through the reticule endothelial system (RES) as the GQDs were not target-specific, and the fluorescence decreased gradually as blood circulated[4]. Based on the excellent synergistic therapeutic performance of the graphene nano-composite systems, detailed long-term retention and *in vivo* toxicity should be investigated in order to confirm their potential for clinical applications[34]. We did not observe either death or a significant decrease in body weight for any of the treatments (Supplementary Figure S8). More importantly, long-term toxicity was evaluated by monitoring histological changes in the most important organs such as the liver, spleen, kidney, heart, and lungs. There was no observable histological lesion or any other adverse effect associated with administration of the nano-materials (Supplementary Figures S9–S14). In addition, the structures of the most important organs in the exposed mice were not different from those in the control groups (Supplementary Figure S9). Based on these results, graphene derivative-Cur nanoparticles appear to be promising candidates for synergistic and safe therapeutic agents.

Discussion

Therefore, according to our experimental result we could conclude that, this is a comprehensive study of cancer therapy using ultrahigh hydrophobic drug-loaded *via* pH dependence of graphene derivatives based on their number of oxygen containing functional groups. GO-Cur, DGO-Cur, and GQD-Cur composites were prepared based on interactions between Cur and the number of oxygen-containing functional groups of the respective starting materials. The drug-

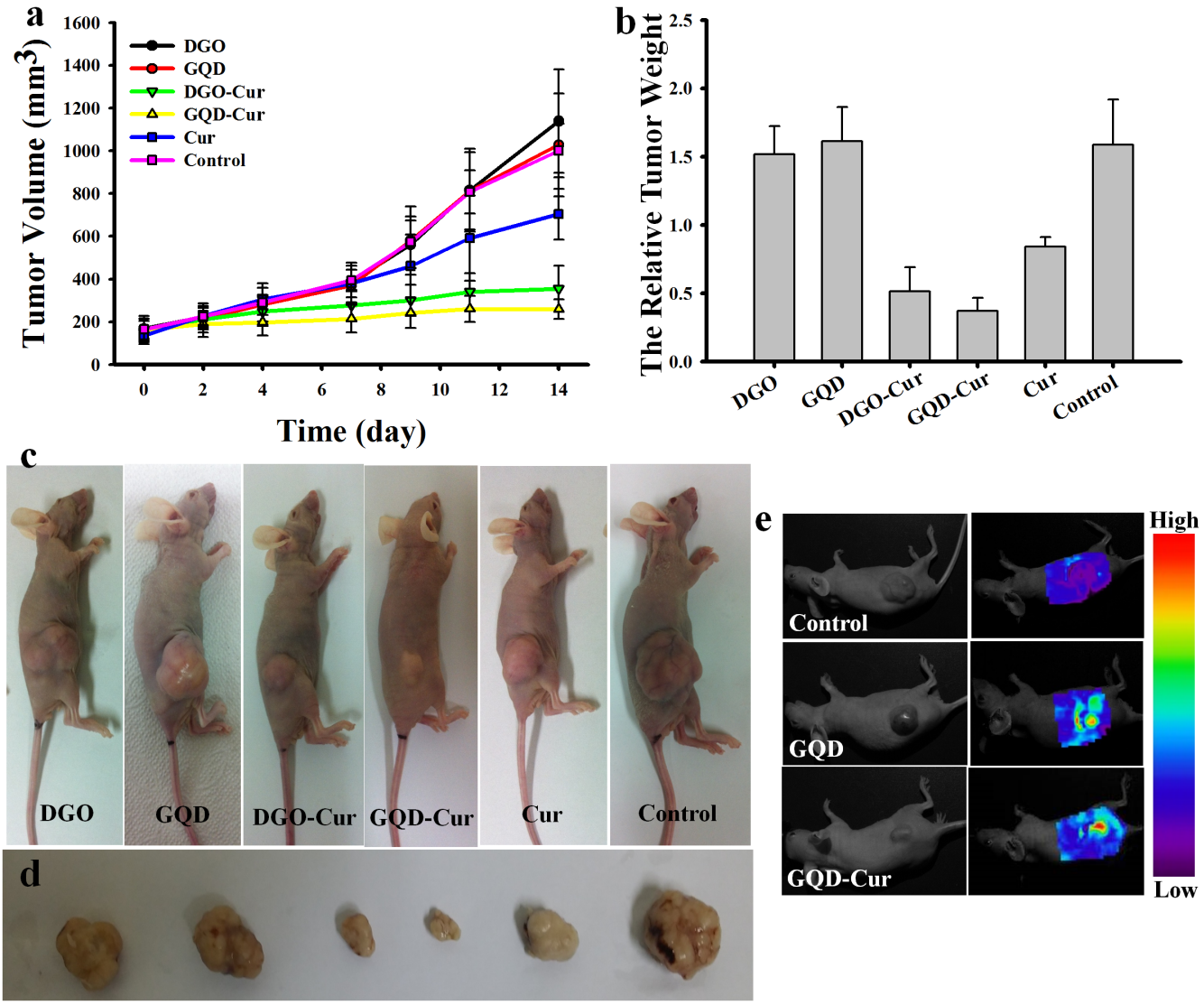

Figure 6 | ***In vivo* experimental data.** (a) Relative tumor volumes of mice (n = 6) treated with PBS, DGO, GQD, DGO-Cur, GQD-Cur, and Cur; (b) Relative tumor weights of mice (n = 6) treated with PBS, DGO, GQD, DGO-Cur, GQD-Cur, and Cur; (c) Photographs of mice treated with PBS, DGO, GQD, DGO-Cur, GQD-Cur, and Cur after 14 days; (d) Photographs of tumors after 14 days of treatment with PBS, DGO, GQD, DGO-Cur, GQD-Cur, and Cur; (e) *in vivo* imaging of tumor-bearing mice after injection of GQDs and GQD-Cur (10 mg/kg).

loading increased with an increasing number of oxygen-containing functional groups of graphene derivatives, which indicated that the oxygen functional groups play a key role in the improvement of hydrophobic drug loading on the surface of graphene. This is the first study to demonstrate pH dependence of ultrahigh hydrophobic drug (Cur) loading by graphene-based nanocariers. Excitingly, the GQDs used in this study exhibited an ultrahigh drug-loading capacity (40,800 mg/g), which is the highest value ever reported for a nanomaterial-based carrier. Our as-made graphene and Cur composites contained the largest amount of Cur nano-particles and had the best anticancer activity in comparison to other composites including Cur alone at the same doses. Many previous studies have reported *in vivo* tumor images after intratumor injection of bio-probe drugs (like DOX); however, in our case, Cur and its GQD composites have no fluorescence, and it is only after the release of Cur from GQD composites that the remaining GQD exhibits a fluorescence signal. Thus, our data provide evidence that the maximum amount of drug was released from the nanoparticles that simultaneous act as a bioprobe for tumour imaging.

In summary, our results show that graphene-based nanocarriers based on the number of oxygen-containing functional groups and delivered in a pH-dependent manner can be used as part of a high-performance hydrophobic drug-delivery platform for the antitumor drug Cur. Of particular significance, the graphene derivative-Cur complexes had an extremely large Cur-loading capacity of 40800 mg/g, which is much higher than that previously reported for nanomaterial-based drug carriers. Among the various graphene derivatives tested, GQD was able to produce a composite and carry large amounts of the drug Cur. *In vitro* experiments revealed that the graphene derivative-Cur complexes facilitated Cur release and efficient cancer cell death. We further demonstrated that Cur-loaded graphene derivatives were highly efficacious in inhibiting tumor growth *in vivo* as mice treated with GQD-Cur or DGO-Cur survived more than 14 days with no detectable tumor growth. At a glance, we have demonstrated a synergistic effect on cancer cell viability both *in vitro* and *in vivo*; the graphene derivative-Cur nano-composite system exhibited the highest anticancer activity among all of the GQD-Cur composites tested, including Cur alone at the same dose. To the best of our knowledge, this is the first example of a synergistic chemotherapeutic agent targeting cancer cells *in vitro* and *vivo* using GQD-Cur composites that also simultaneously act as a superficial bioprobe for tumor imaging. Given that graphene derivatives can be readily produced with relatively high yield and low cost, graphene-based nanocarriers may serve as a practical and powerful tool for cancer therapy, rivalling or complementing current state-of-the-art nanomaterial-based nanocarriers. With its superior stability, high biocompatibility, and excellent synergistic therapy performance, this drug-delivery system may be a promising *in vivo* cancer therapy agent. This study significantly advances our knowledge of the biological properties of Cur and graphene composites and their use in biomedical and biotechnological applications. Furthermore, we are currently investigating these composites for application in HIV treatment, as well as that for neurological, cardiovascular, and skin diseases.

Methods

Preparation of graphene oxides (GOs). GO sheets were prepared from natural graphite powder using the modified Hummer's method with sulfuric acid, potassium permanganate, and sodium nitrate[23].

Synthesis of double-oxidized graphene oxide (DGO). DGO sheets were synthesized according to our reported procedure for as-made GO[24].

Synthesis of graphene quantum dots (GQD). Oxygen-containing GQDs were synthesized as described previously[4].

Synthesis of GO-Cur, DGO-Cur, and GQD-Cur composites. GO, DGO, and GQD nanosheets were dispersed in deionized distilled water (~200 μg/mL), and the solution was adjusted to pH ~ 9, and finally, five times the amount of Cur w.r.f. to GO, DGO and GQD was mixed in the solutions. The reaction mixture was then stirred at 4°C for 30 min followed by centrifugation at 14,000 rpm for 20 min and washing three times with DI water, and the resulting pellet was dried under vacuum. In addition, GQD-Cur was collected by recrystallization of unattached Cur and evaporation of the resulting solution.

The drug-loading capacity was determined as $(W_{\text{initial Cur}} - W_{\text{Cur in excess}})/(W_{\text{graphene-derivatives}})$ $(\text{mg/g})^2$, where $W_{\text{initial Cur}}$ is the initial weight of Cur added, $W_{\text{Cur in excess}}$ is the weight of Cur in the supernatant, and $W_{\text{graphene derivatives}}$ is the weight of graphene derivatives (GO, DGO and GQD). The weight of excess Cur was 184 μg at pH = 9 and Cur concentration = 1000 μg/mL, and thus the weight of Cur loaded on the QGD was 816 μg. As a result, the loading capacity of Cur on GQD was 40800 mg/g for 1 mg of Cur, while the concentration of Cur loaded on the GO and DGO was 20800 mg/g and 38800 mg/g, respectively, at pH = 9. Graphene derivative-Cur complexes prepared at pH = 9 were re-suspended in DI water at different pH values (5, 7.5, and 9) for different times (5, 10, 15, 20 and 24 h) at room temperature. The number of Cur molecules that remained on the graphene derivative surfaces was calculated based on the weight of released Cur.

Cell culture. Human colon cancer cells (HCT116) were maintained in Dulbecco's modified Eagle's medium (DMEM), supplemented with 10% fetal bovine serum (FBS) and antibiotics (10,000 μg/mL streptomycin and 10,000 unit/mL penicillin) at 37°C in a humidified atmosphere containing 5% CO_2 (v/v).

Cytotoxicity assay. *In vitro* cytotoxicity was measured using a standard colorimetric 3-(4, 5-dimethylthiazol-2-yl)-2, 5-diphenyl tetrazolium bromide (MTT) assay. For the MTT assay, HCT116 cells were seeded in a 96-well cell-culture plate at 1×10^4/well and incubated for 12 h at 37°C under 5% CO_2. Afterwards, HCT116 cells were incubated for 24 h with various concentrations (from 6.125, 12.5, 25, 50, and 100 μg/mL) of GO, DGO, GQD, Cur, GO-Cur, DGO-Cur, and GQD-Cur by diluting stock solutions with PBS. Next, 20 μL of MTT (5 mg/mL) was added to each well, and cells were incubated for 4 h at 5% CO_2 and 37°C. After incubation for another 4 h, the resultant formazan crystals were dissolved in dimethyl sulfoxide (DMED, 100 μl), and the absorbance intensity was measured by a microplate reader at 570 nm. All experiments were performed in quadruplicate, and the relative cell viability (%) was expressed as a percentage relative to untreated control cells.

Flow cytometric analysis. 2×10^5 HCT116 cells/well in 6-well plates were cultured with PBS, GO, DGO, GQD, Cur, GO-Cur, DGO-Cur and GQD-Cur for 24 h. Cell death population was measured by flow cytometry (BD FACSCalibur, BD biosciences, USA) using an apoptosis detection kit (BD Pharmingen, San Diego) according to the manufacturer's protocols. Briefly, harvested cells were stained with FITC conjugated anti-Annexin V Abs and propidium iodide (PI) for 15 min. Early apoptotic (Annexin V-positive, PI-negative), late apoptotic (Annexin V-positive and PI-positive) and necrotic (Annexin V-negative and PI-positive) cells were included in total cell death determinations.

Immunofluorescence. For 4,6-diamidino-2-phenylindole (DAPI) staining, cells were grown on glass coverslips until 80% confluence was reached. The cells were then washed with PBS, fixed in methanol (−20°C) for 2 min, and stained with 1 mM DAPI for 5 min in the dark. After washing with PBS, nuclear morphology was analysed by fluorescence microscopy.

***In vivo* drug delivery.** Six- to seven-week-old Balb/c female nude mice (weight range of 21–25 g) were purchased from Orient Bio Inc. (Seoul, Korea) and were maintained on a 12-h light/12-h dark cycle (12 : 12LD) at a room temperature of 23 ± 1°C, humidity 40–60%, and with food and water *ad libitum*. Human colon cancer cells (HCT116) were trypsinized, washed twice with serum-free DMEM, and suspended at a density of 1×10^7 cells/mL PBS. An amount of 100 μL of the suspended cells was subcutaneously injected into the right back region of the mice. After the tumor size reached about 150 mm^3, the mice were randomly divided into six groups, minimizing weight and tumor size differences. The mice were intratumorally administered with physiological saline, DGO, GQD, Cur, DGO-Cur and GQD-Cur suspensions at a total dose of 5 and 10 mg/kg. The tumor size of each group was measured using a caliper, and tumor volume was calculated using the following equation: tumor volume = $ab^2 \times 0.5236$, where 'a' the maximum diameter of tumor and 'b' is the minimum diameter of tumor. Relative tumor volumes were calculated as V/V_0 (V_0 was the tumor volume when the treatment was initiated). All experiments were performed in accordance with relevant guidelines and regulations, was approved by the Ethical Committee on Animal Experimentation at Sungkyunkwan University.

Noninvasive optical imaging study. After 14 days, tumor-bearing mice were intratumorally receiving 10 mg/kg of the composites. Mice were anesthetized with ketamine (87 mg/kg) and xylazine (13 mg/kg) *via* intraperitoneal (IP) injection. Noninvasive images of the GQD-Cur, only GQD and PBS, injected mice were taken by an optical tomography system. Mice were placed on the imaging platform, and images were taken at 4 h post-injection. The 3D scanning region of interest was selected using a bottom-view charge-coupled device (CCD). All images were taken using the Optix *in vivo* imaging system (Optix MX3, ART Advanced Research Technologies INC, Canada).

Histology analysis. For histology studies, mice were sacrificed for two weeks after administration. The tissues (heart, spleen, liver, lung and kidney) were collected from

each group and fixed in 10% formalin and embedded in paraffin. Multiple 4 μm-thick microtome sections from tissues were stained with hematoxylin and eosin (H&E). The histological sections were observed under an optical microscope.

1. Liu, Z., Sun, X., Nakayama-Ratchford, N. & Dai, H. Supramolecular chemistry on water-soluble carbon nanotubes for drug loading and delivery. *ACS Nano* **1**, 50–56 (2007).
2. Peng, F. *et al.* Silicon-nanowire-based nanocarriers with ultrahigh drug-loading capacity for in vitro and in vivo cancer therapy. *Angew. Chem. Int. Ed.* **52**, 1457–1461 (2013).
3. Liu, Z., Robinson, J. T., Sun, X. M. & Dai, H. J. PEGylated nanographene oxide for delivery of water-insoluble cancer drugs. *J. Am. Chem. Soc.* **130**, 10876–10877 (2008).
4. Nurunnabi, M. *et al.* In vivo biodistribution and toxicology of carboxylated graphene quantum dots. *ACS Nano* **7**, 6858–6867 (2013).
5. Nahain, A. *et al.* Target delivery and cell imaging using hyaluronic acid-functionalized graphene quantum dots. *Mol. Pharmaceutics* **10**, 3736–3744 (2013).
6. Hu, C.-M. J. & Zhang, L. Therapeutic nanoparticles to combat cancer drug resistance. *Curr. Drug Metab.* **10**, 836–841 (2009).
7. Jabr-Milane, L. S., van Vlerken, L. E., Yadav, S. & Amiji, M. M. Multi-functional nanocarriers to overcome tumor drug resistance. *Cancer Treat. Rev.* **34**, 592–602 (2008).
8. Shen, H., Zhang, L., Liu, M. & Zhang, Z. Biomedical applications of graphene. *Theranostics* **2**, 283–294 (2012).
9. Zhang, L. M. *et al.* Functional graphene oxide as a nanocarrier for controlled loading and targeted delivery of mixed anticancer drugs. *Small* **6**, 537–544 (2010).
10. Sahoo, N. G. *et al.* Functionalized carbon nanomaterials as nanocarriers for loading and delivery of a poorly water-soluble anticancer drug: a comparative study. *Chem. Commun.* **47**, 5235–5237 (2011).
11. Feng, L. Z. & Liu, Z. A. Graphene in biomedicine: opportunities and challenges. *Nanomedicine* **6**, 317–324 (2011).
12. Bao, H., Pan, Y. & Li, L. Recent advances in graphene-based nanomaterials for biomedical applications. *Nano Life* **02**, 1230001–1230015 (2012).
13. Liu, C. *et al.* Graphene-based anticancer nanosystem and its biosafety evaluation using a zebrafish model. *Biomacromolecules* **14**, 358–366 (2013).
14. Arayachukeat, S., Palaga, T. & Wanichwecharungruang, S. P. Clusters of carbon nanospheres derived from graphene oxide. *ACS Appl. Mater. Interfaces* **4**, 6808–6815 (2012).
15. Wang, Z. *et al.* Synthesis of strongly green-photoluminescent graphene quantum dots for drug carrier. *Colloids Surf. B-Biointerfaces* **112**, 192–196 (2013).
16. Wang, C. *et al.* Enhancing cell nucleus accumulation and DNA cleavage activity of anti-cancer drug via graphene quantum dots. *Sci Rep.* **3**, 2852–2860 (2013).
17. Sanchez, V. C., Jachak, A., Hurt, R. H. & Kane, A. B. Biological interactions of graphene-family nanomaterials: an interdisciplinary review. *Chem. Res. Toxicol.* **25**, 15–34 (2011).
18. Lee, D. Y., Khatun, Z., Lee, J. H., Lee, Y. K. & In, I. Blood compatible graphene/heparin conjugate through noncovalent chemistry. *Biomacromolecules* **12**, 336–341 (2011).
19. Grigoryan, G. *et al.* Computational design of virus-like protein assemblies on carbon nanotube surfaces. *Science* **332**, 1071–1076 (2011).
20. Yang, K., Feng, L., Shi, X. & Liu, Z. Nano-graphene in biomedicine: theranostic applications. *Chem. Soc. Rev.* **42**, 530–547 (2013).
21. Yang, K., Li, Y., Tan, X., Peng, R. & Liu, Z. Behavior and toxicity of graphene and its functionalized derivatives in biological systems. *Small* **9**, 1492–1503 (2013).
22. Wu, J. *et al.* Graphene oxide used as a carrier for adriamycin can reverse drug resistance in breast cancer cells. *Nanotechnology* **23**, 355101–355110 (2012).
23. Some, S. *et al.* Can commonly used hydrazine produce n-type graphene? *Chem. A Eur. J.* **18**, 7665–7670 (2012).
24. Hong, B. J., Compton, O. C., An, Z., Eryazici, I. & Nguyen, S. T. Successful stabilization of graphene oxide in electrolyte solutions: enhancement of biofunctionalization and cellular uptake. *ACS Nano* **1**, 63–73 (2012).
25. Some, S. *et al.* Dual functions of highly potent graphene derivative-poly-L-lysine composites to inhibit bacteria and support human cells. *ACS Nano* **8**, 7151–7161 (2012).
26. Mohan, P. R. K., Sreelakshmi, G., Muraleedharan, C. V. & Joseph, R. Water soluble complexes of curcumin with cyclodextrins: characterization by FT-raman spectroscopy. *Vib. Spectrosc.* **62**, 77–84 (2012).
27. Leung, M. H. M., Colangelo, H. & Kee, T. W. Encapsulation of curcumin in cationic micelles suppresses alkaline hydrolysis. *Langmuir* **24**, 5672–5675 (2008).
28. Peng, J. *et al.* Graphene quantum dots derived from carbon fibers. *Nano lett.* **12**, 844–849 (2012).
29. Mathew, A. *et al.* Curcumin loaded-PLGA nanoparticles conjugated with tet-1 peptide for potential use in alzheimer's disease. *PLoS ONE* **7**, 32616–32626 (2012).
30. Zhu, S. *et al.* Graphene quantum dots with controllable surface oxidation, tunable fluorescence and up-conversion emission. *RSC Advances* **2**, 2717–2720 (2012).
31. Patra, D. & Sleem, F. A new method for pH triggered curcumin release by applying poly(l-lysine) mediated nanoparticle-congregation. *Anal. Chim. Acta* **795**, 60–68 (2013).
32. Wang, P., Yu, J. & Zhang, L. The nuclear function of p53 is required for PUMA-mediated apoptosis induced by DNA damage. *Proc. Natl. Acad. Sci. U. S. A.* 2007 **104**, 4054–4059 (2007).
33. Mobasher, M. A. *et al.* Protein tyrosine phosphatase 1B modulates GSK3β/Nrf2 and IGFIR signaling pathways in acetaminophen-induced hepatotoxicity. *Cell Death & Disease* **4**, 626–639 (2013).
34. Yang, Y. *et al.* Long-term in vivo biodistribution and toxicity of $Gd(OH)_3$ nanorods. *Biomaterials* **34**, 508–515 (2013).

Acknowledgments

This work was supported by the National Research Foundation of Korea (NRF) grant funded by the Korean government (MSIP) (Grant No. 2006-0050684) and Basic Science Research Program (grant number 2013063062).

Author contributions

S.S. and H.L. wrote the manuscript. S.S. prepared and characterized all materials. A.G., G.B., S.K. and D.J. performed bio-experiments. E.H., S.B. and J.Y. prepared graphene quantum dots. Y.Y. and Y.K. prepared gaphene oxide and double oxidized graphene oxide. H.L. and S.S. supervised the work.

Additional information

Supplementary information accompanies this paper at http://www.nature.com/scientificreports

Competing financial interests: The authors declare no competing financial interests.

How to cite this article: Some, S. *et al.* Cancer Therapy Using Ultrahigh Hydrophobic Drug-Loaded Graphene Derivatives. *Sci. Rep.* **4**, 6314; DOI:10.1038/srep06314 (2014).